JOURNAL OF VIROLOGY, May 1997, p. 4032–4041 Vol. 71, No. 5
0022-538X/97/$04.00+0
Copyright © 1997, American Society for Microbiology

A Novel Virus Binding Assay Using Confocal Microscopy: Demonstration that the Intracellular and Extracellular Vaccinia Virions Bind to Different Cellular Receptors

ALAIN VANDERPLASSCHEN AND GEOFFREY L. SMITH*

Sir William Dunn School of Pathology, University of Oxford, Oxford OX1 3RE, United Kingdom

Received 6 December 1996/Accepted 30 January 1997

Vaccinia virus (VV) produces two antigenically and structurally distinct infectious virions, intracellular mature virus (IMV) and extracellular enveloped virus (EEV), which bind to unidentified and possibly different cellular receptors. Studies of VV binding have been hampered by having two infectious virions and by the rupture of the EEV outer membrane in the majority of EEV virions during purification. To overcome these problems, we have developed a novel approach to study VV binding that is based on confocal microscopy and does not require EEV purification. In this assay, individual virus particles adsorbed to the cell are simultaneously distinguished and quantified by double immunofluorescence labelling with antibody markers for EEV and IMV. By this method, we show unequivocally that IMV and EEV bind to different cellular receptors. Three independent observations allow this conclusion. First, the efficiencies with which IMV and EEV bind to different cell lines are unrelated; second, cell surface digestion with some enzymes affects IMV and EEV binding differently; and third, the binding of a monoclonal antibody to cells prevents IMV binding but not EEV binding. This technique may be widely applicable for studying the binding of different viruses.

Vaccinia virus (VV) is a poxvirus and produces large (250- by 350-nm) and complex virions that contain a double-stranded DNA genome and more than 100 polypeptides (8). There are two morphologically distinct infectious forms of virions, intracellular mature virus (IMV) and extracellular enveloped virus (EEV) (2, 10). IMV represents the majority of infectious progeny and remains within the cytoplasm of the infected cell until cell lysis. EEV is released from the cell and possesses an extra lipid envelope with at least 10 associated proteins which are absent from IMV (14, 15). These proteins endow EEV with different biological and immunological properties (2–4, 19). Despite the fact that EEV constitutes only a very minor fraction of total infectivity, it has two important biological properties. First, it mediates long-range dissemination of virus both in vitro and in vivo (15); second, it is the form of virus against which immune responses that are necessary for protection against infection by orthopoxviruses are induced (1, 3, 15).

Because EEV has an extra lipid envelope containing proteins absent from IMV, it is possible that each form of VV binds to distinct cellular receptors and consequently could have different tropisms. Surprisingly, this question, which is important for the understanding of VV pathogenesis and for the use of VV as a live recombinant vaccine, has not been investigated so far. Recently, Chang et al. described the isolation of a mouse immunoglobulin M (IgM) monoclonal antibody (MAb), B2, which reacts with a trypsin- and pronase-sensitive and neuraminidase-resistant cell surface epitope (5). When bound on the cell surface, MAb B2 was shown to prevent IMV binding, but its effect on EEV binding or infectivity was not tested.

Binding studies require purified virus, and this is particularly true for VV, which produces two forms of infectious virions. Despite the fact that EEV is the only form actively released from the cell, the supernatant of infected cells cannot be used as a source of pure EEV because it contains contaminating IMV released from lysed cells. Furthermore, because IMV is much more abundant than EEV (≥100-fold for the Western Reserve strain), breakage of only a minor proportion of cells produces overwhelming contamination. Recently, Ichihashi has shown that biophysical methods to separate EEV from IMV cause damage to the outer envelope of EEV virions, as demonstrated by their sensitivity to MAbs that neutralize IMV (9). Once the EEV membrane is ruptured, the particle retains full infectivity as an IMV. Similarly, if the EEV envelope presents a defect which reduces the specific infectivity of EEV virions, the rupture of the EEV membrane increases the specific infectivity (12). Because damaged EEV could bind to the cell via an EEV or IMV protein, purified EEV should not be used for binding studies.

To overcome these difficulties, we have developed a novel binding assay based on confocal microscopy which does not require purified virions. By this assay, we demonstrate that IMV and EEV bind to different cellular receptors. This method should be applicable for studying many different viruses.

MATERIALS AND METHODS

Cells and viruses. BS-C-1 cells (African green monkey kidney cells; ATCC CCL-26) and RK_{13} cells (rabbit kidney cells; ATCC CCL-37) were grown in minimum essential medium (MEM) (Gibco) supplemented with 10% fetal bovine serum (FBS). HeLa cells (ATCC CCL-10) were grown as suspension cultures as described elsewhere (6).

The International Health Department-J VV strain, which produces large amounts of EEV, was grown in RK_{13} cells infected with 1 PFU per cell. Three virus preparations were produced from the infected cultures. For fresh EEV, the culture supernatant was harvested at 24 h after infection and centrifuged to remove detached cells and cell debris (1,000 × *g*, 20 min, 4°C). A fresh EEV preparation was produced before each experiment. Alternatively, 48 h after infection, IMV and EEV were purified as described previously (13). Purified IMV and EEV were stored at −70°C and were sonicated at 40 μm for 30 s before use. Virus infectivity was titrated by plaque assay with BS-C-1 cells. Unless otherwise specified, cells were incubated with serial dilutions of the virus in phosphate-buffered saline (PBS) (3 mM KCl, 1.5 mM KH_2PO_4, 0.14 M NaCl, 6.5 mM Na_2HPO_4 [pH 7.2]) containing 2% FBS (0.5 ml per well of 6-well cluster

* Corresponding author. Mailing address: Sir William Dunn School of Pathology, University of Oxford, South Parks Rd., Oxford OX1 3RE, United Kingdom. Phone: 44-1865-275521. Fax: 44-1865-275501. E-mail: geoffrey.smith@path.ox.ac.uk.

Downloaded from http://jvi.asm.org/ on September 15, 2019 by guest

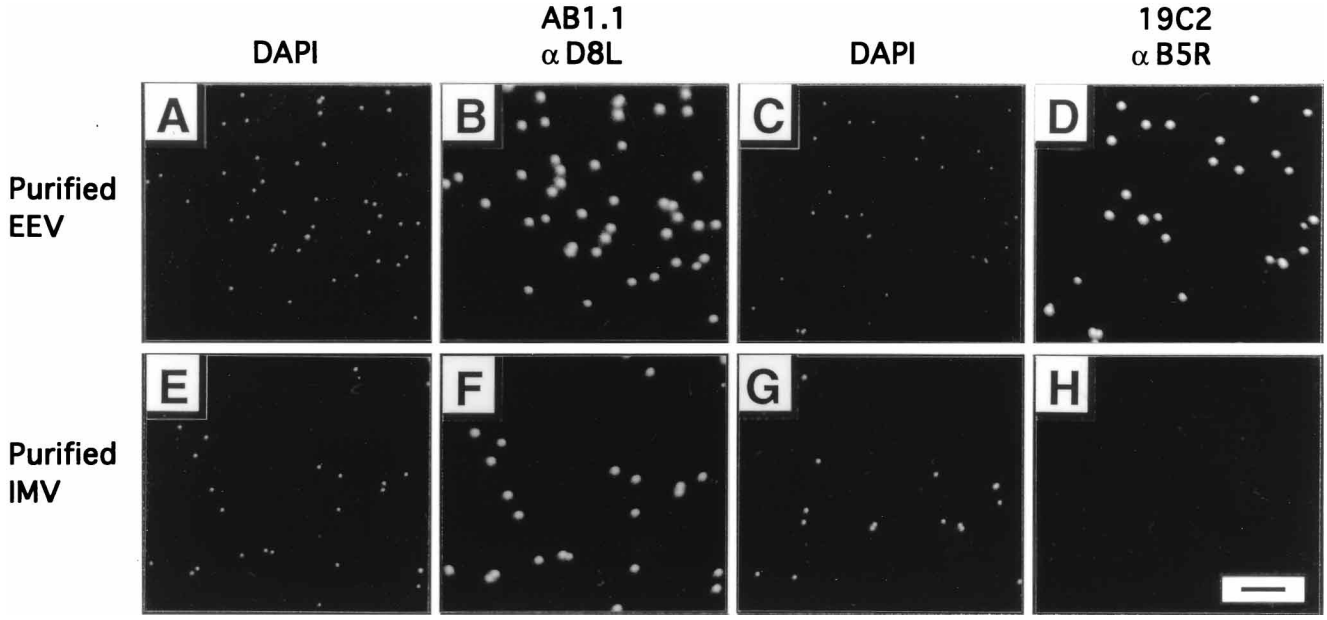

FIG. 1. Visualization of IMV and EEV by conventional fluorescent microscopy. Purified EEV (A through D) and IMV (E through H) (10^7 PFU/ml in PBS) were incubated for 30 min at 37°C on the surface of glass coverslips coated with fibronectin. After being washed with PBS, the virions adsorbed to fibronectin were treated as described in Materials and Methods for indirect immunofluorescent staining. MAb AB1.1 (B and F) and MAb 19C2 (D and H) were used as primary antibodies and were revealed by FITC-GAM and FITC-RAR secondary antibodies, respectively. The samples were then examined with a conventional fluorescent microscope (magnification, ×1,000; Axioplan microscope; Zeiss). Panel pairs (A and B, C and D, E and F, and G and H) represent the same field examined for DAPI and FITC fluorescent emissions, respectively. Bar, 2 μm. αD8L, anti-D8L; αB5R, anti-B5R.

dishes) for 1 h at 4°C, washed with PBS–2% FBS, and overlaid with 1.5% carboxymethyl cellulose (CMC) in MEM with 2.5% FBS (11). After 2 days, cells were stained with 0.1% crystal violet in 15% ethanol and the plaques were counted. To determine only the infectivity associated with EEV, any contaminating IMV infectivity was neutralized by the addition of MAb 5B4/2F2 (final dilution, 1/2,560) against the 14-kDa fusion protein (A27L gene product) of IMV (7).

MAbs. Culture supernatant from a murine hybridoma secreting the IgM MAb B2 was kindly provided by W. Chang (5). Murine MAb AB1.1 (13), raised against the D8L IMV surface protein, and rat MAb 19C2 (18), raised against the B5R EEV surface protein, were also used.

Capping of the MAb B2-reactive epitope. Capping of the MAb B2-reactive epitope was induced in HeLa cells grown as suspension cultures. Cells (10^6) were incubated for 1 h on ice with 0.2 ml of MAb B2-undiluted supernatant. Then cells were washed with cold PBS–10% FBS (PBSF) and further incubated for 30 min on ice with a rabbit antiserum to mouse IgM (RAM-IgM; Serotec) (16 μg/10^6 cells in 0.2 ml of PBSF). After washing with cold PBSF, capping was induced by incubation at 37°C for 10 min followed by cooling to 0°C to stop the process.

Cell surface enzymatic digestions. Trypsin (1.25 mg/ml; from bovine pancreas; Boehringer Mannheim), pronase (1 mg/ml; from *Streptomyces griseus*; Boehringer Mannheim), and neuraminidase (40 mU/ml; from *Vibrio cholerae*; Boehringer Mannheim) digestions were carried out in PBS for 30 min on ice. Cells were then washed extensively with cold PBS–2% FBS.

Indirect immunofluorescent staining for conventional microscopy and confocal microscopy. Virus particles bound to fibronectin-coated coverslips or cells were fixed in PBS containing 4% paraformaldehyde (wt/vol) for 20 min on ice. After being washed with PBS, samples were permeabilized in ethanol-PBS (90:10 [vol/vol]) at 0°C for 2 min. Then samples were extensively washed with PBS and incubated in PBSF containing the appropriate concentration of the primary MAb at 37°C for 45 min. MAb AB1.1 (diluted 1/300), biotinylated MAb AB1.1 (diluted 1/100), or MAb 19C2 (diluted 1/16) was used as the primary antibody. After being washed with PBSF, samples were incubated in PBSF containing the appropriate secondary reagent at 37°C for 30 min. Fluorescein isothiocyanate (FITC)-conjugated $F(ab')_2$ goat anti-mouse IgG (GAM) (8 μg/ml) (Sigma), rhodamine-conjugated streptavidin (Rd-Strep) (3.3 μg/ml) (Serotec), and FITC (10 μg/ml) (Serotec)- or *R*-phycoerythrin (PE) (10 μg/ml) (Serotec)-conjugated $F(ab')_2$ rabbit anti-rat IgG (RAR) were used as secondary conjugates, respectively. After extensive washing with PBSF and a final wash step with distilled water, samples were mounted in Mowiol-DAPI (6-diamin-2-phenylindole-dihydrochloride) mounting medium as described elsewhere (17). This mounting medium contained 1 μg of DAPI per ml.

Quantification of cell surface MAb B2-reactive epitope by indirect immunofluorescent staining and flow cytometry. HeLa cells (10^6) grown as suspension cultures were incubated for 1 h on ice in 0.2 ml of MAb B2 pure supernatant or in 0.2 ml of PBSF containing a mouse isotype IgM negative control (10 μg/10^6 cells) (Serotec). After being washed with cold PBSF, cells were further incubated with a FITC-conjugated sheep antiserum to mouse IgM (SAM-IgM) (Serotec) (16 μg/10^6 cells in 0.2 ml of PBSF) on ice for 30 min. After being washed with cold PBSF, cells were fixed in PBS containing 4% formaldehyde (vol/vol) and analyzed by flow cytometry.

Confocal-microscopy analysis. Cells were analyzed with a Bio-Rad MRC 1000 confocal microscope (run with Comos software) by using appropriate filters, the full dynamic range of grey scale, and Kalman filtration. Optical sections perpendicular to the z axis were performed every 0.6 μM throughout the sample. The confocal pictures were reconstructed by projection of sections.

Flow cytometry analysis. Flow cytometry analysis for FITC emission signal was performed with a FACScan flow cytometer (Becton Dickinson) as described previously (20).

Statistical analysis. Student's *t* test was used to test the significance of results ($P < 0.05$).

RESULTS

IMV and EEV particles can be visualized by conventional fluorescent microscopy. VV is a very large virus (approximately 250 by 350 nm); therefore, we investigated whether indirect immunofluorescent staining could be used as a novel assay to study VV binding to cells. Purified IMV and EEV (10^7 PFU/ml in PBS) were first incubated for 30 min at 37°C on the surface of glass coverslips coated with fibronectin. After being washed with PBS, adsorbed virions were treated as described in Materials and Methods for indirect immunofluorescent staining with MAb AB1.1 (anti-D8L gene product) (Fig. 1B and F) or MAb 19C2 (anti-B5R gene product) (Fig. 1D and H). Staining of viral DNA with DAPI enabled each isolated IMV and EEV particle to be visualized (Fig. 1A, C, E, and G). A much brighter signal was observed when virions (IMV or EEV) were revealed by indirect immunofluorescent staining. As expected, both IMV and EEV permeabilized particles were stained by MAb AB1.1 directed against the IMV surface protein D8L. Importantly, all the virions detected by DAPI staining were also revealed by staining with MAb AB1.1 (Fig. 1; compare

Downloaded from http://jvi.asm.org/ on September 15, 2019 by guest

panels A and B and panels E and F). In contrast, MAb 19C2, which recognizes only EEV particles (18), stained 3% of the purified IMV particles revealed by DAPI staining ($n = 400$), indicating that the majority of the virions of this preparation were IMV (Fig. 1; compare panels G and H). Consistent with this, 95% ($n = 598$ PFU in the absence of MAb 5B4/2F2) of the purified IMV PFU were neutralized by MAb 5B4/2F2. Taken together, these data indicate the reasonably high purity of the purified IMV preparation and the efficiency with which MAb 5B4/2F2 neutralizes IMV infectivity.

For the purified EEV preparation, 96% of virions were stained by MAb 19C2 (determined by observation of 400 DAPI-positive particles), indicating that the majority of the virions of this preparation were EEV. When purified EEV was submitted to neutralization assay with MAb 5B4/2F2, 65% ($n = 453$ PFU in the absence of MAb 5B4/2F2) of the PFU were neutralized. Taking into account that only 31% of the infectivity of the original culture supernatant used for EEV purification was neutralized by MAb 5B4/2F2, these data indicated that the purification procedure led to isolation of EEV with a damaged outer membrane, allowing access of IMV-neutralizing antibody. Despite several attempts using different protocols, we were not able to purify EEV without obtaining a large fraction of damaged particles. Therefore, all further investigations on EEV biology were carried out with fresh EEV prepared at 24 h postinfection from the cell supernatant. For EEV infectivity assays, any contaminating IMV was neutralized by the addition of MAb 5B4/2F2. For binding studies, we developed a double immunofluorescent staining which permits IMV and EEV bound on the cell surface to be counted and differentiated simultaneously.

Simultaneous identification of IMV and EEV on the cell surface by double immunofluorescent staining and confocal microscopy analysis. Fresh EEV contains 15 to 25% contaminating IMV; therefore, its use for binding studies requires an assay which permits differentiation of IMV and EEV. With that goal in mind, we used a double immunofluorescent staining with MAbs AB 1.1 and 19C2 against the D8L and B5R gene products, respectively, on fixed and permeabilized samples (Fig. 2). Biotinylated MAb AB1.1 and MAb 19C2 were used as primary MAbs and were subsequently revealed by Rd-Strep and FITC-RAR, respectively. By this staining procedure, EEV virions appeared as double (red and green) foci while IMV virions were single (red) fluorescent foci on the cell surface. Each fluorescent focus was shown to represent an isolated particle and not a virus cluster by measuring the sizes of spots. The mean diameter of Rd fluorescent foci was 409.3 nm (standard deviation [SD] = 13.1; $n = 20$), which is similar to the dimension of a single vaccinia virion. This also demonstrated that the virus preparations contained disaggregated particles.

Determination of physical particle/PFU ratios. The ability to visualize individual VV virions and to determine their phenotypes by double immunofluorescent staining provided a simple way to determine the numbers of EEV and IMV particles per volume unit. To do this, the VV preparation whose titer was to be determined was serially diluted in distilled water. One microliter of each dilution was then loaded in triplicate on the surface of a glass coverslip coated with fibronectin (washed with distilled water and dried beforehand). After being dried completely, virions were fixed to fibronectin with 4% paraformaldehyde in PBS for 30 min on ice. Then samples were permeabilized and treated for double immunofluorescent staining as described above. The numbers of EEV (double-positive) and IMV (single-positive) particles were then counted on the entire area corresponding to each drop from dilutions giving between 100 and 1,000 virions/drop. The mean number of the three measurements multiplied by the dilution factor enabled the number of EEV or IMV virions/ml to be calculated. Simultaneously, the total infectivity (EEV plus IMV) was determined by plaque assay with BS-C-1 cells in triplicate and the infectivity associated with EEV was determined by plaque assay in the presence of MAb 5B4/2F2. To ensure that all the infectious particles had sufficient time to bind to cells, the virus was adsorbed for 3.5 h at 37°C (0.5 ml per well of 6-well cluster dishes). The particle/PFU ratio of IMV was calculated from analyses of purified IMV and fresh EEV, while the EEV particle/PFU ratio was calculated by analysis of fresh EEV. The data given are the means from three independent virus preparations. The IMV particle/PFU ratios were 45 (SD = 11.1; $n = 3$) and 64.6 (SD = 16.5; $n = 3$) in fresh EEV and purified IMV, respectively. The EEV particle/PFU ratio of fresh EEV was 12.7 (SD = 6.1; $n = 3$). These data indicate that EEV has a higher specific infectivity than does IMV under the conditions tested and that the purification of IMV reduces the specific infectivity.

Cell surface protease treatment affects differently IMV and EEV binding. The binding assay described above enables the identification and differentiation of IMV and EEV bound to the cell surface and consequently allows the use of virus preparations containing both IMV and EEV for binding studies. Therefore, it can be applied to investigate simultaneously the effects of a specific treatment on IMV and EEV binding. We used this feature of the binding assay to investigate whether IMV and EEV bind to identical or separate receptors.

If IMV and EEV bind to separate cellular receptors and these receptors have different biochemical compositions, cell surface treatment with some enzymes might affect differently IMV and EEV binding. To test this hypothesis, we investigated whether treating cells with different enzymes affected differentially IMV and EEV binding and infectivity. Binding and infectivity assays were performed concurrently with RK_{13} and BS-C-1 cells. Binding assays were also performed with HeLa cells grown in suspension. Cell surface treatments with trypsin, pronase, and neuraminidase were carried out as described in Materials and Methods. It was not possible to use BS-C-1 cells for protease experiments due to their high sensitivities to these enzymes causing detachment from the culture vessel.

Trypsin digestion did not affect either IMV binding or infectivity (Table 1). Statistically similar numbers of IMV particles were counted on the surfaces of cells digested with trypsin and those that were mock treated (Table 1). This observation was made with both RK_{13} and HeLa cells and with both sources of IMV (purified IMV and fresh EEV). When RK_{13} cells were subjected to the infectivity assay with purified IMV as the inoculum, similar numbers of PFU were observed for mock- and trypsin-treated cells (Table 1). Surprisingly, and in contrast to IMV, EEV bound more efficiently to trypsin-treated cells than to normal cells. The number of EEV counted on trypsin-treated cells was 2.0 times that observed on control cells. Similarly, EEV generated 2.3 times more plaques on trypsin-treated RK_{13} cell monolayers than on mock-treated monolayers (Table 1).

Pronase treatment had opposite effects on IMV and EEV binding. Pronase treatment of RK_{13} and HeLa cells reduced the amount of IMV bound on the cell surface by 92 and 97%, respectively (Table 1 [purified IMV used as the inoculum]). Similarly, when RK_{13} cell monolayers were treated with pronase before infection, the number of IMV plaques was decreased by 90% in comparison with the control (Table 1). In contrast to IMV, cell surface pronase treatment enhanced EEV binding and infectivity. RK_{13} and HeLa cells treated with

Downloaded from http://jvi.asm.org/ on September 15, 2019 by guest

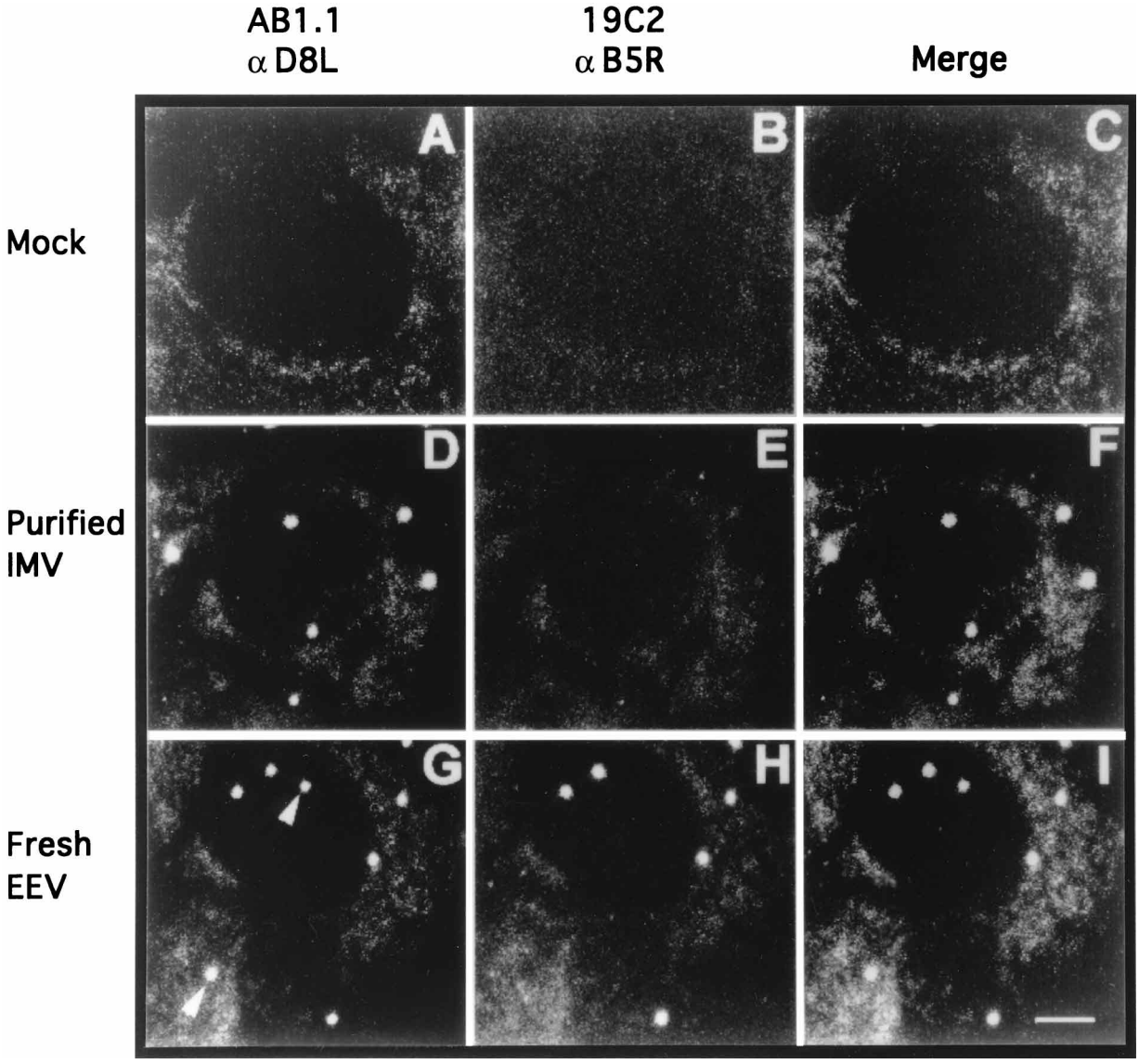

FIG. 2. Detection and identification of IMV and EEV on the cell surface by double immunofluorescent staining and confocal microscopy. RK_{13} cells were mock infected (A through C) or infected on ice with purified IMV (D through F) or fresh EEV (G through I). Cells were then treated as described in Materials and Methods for simultaneous detection of D8L and B5R gene products by double indirect immunofluorescent staining. Biotinylated MAb AB1.1 and MAb 19C2 were used as primary MAbs and were revealed by Rd-Strep and FITC-RAR, respectively. All three panels horizontally analyze the same cells. The first (A, D, and G) and second (B, E, and H) columns of panels are analyses for Rd and FITC fluorescent emissions, respectively. In the third (C, F, and I) column Rd and FITC signals are merged. The arrowheads in panel G identify particles (IMV) which were detected by MAb AB1.1 but not by MAb 19C2. Bar, 2 μm. αD8L, anti-D8L; αB5R, anti-B5R.

pronase bound 2.94 and 2.72 times more EEV, respectively, than did control cells (Table 1). The results of infectivity assays led to a similar conclusion: the number of PFU observed after EEV infection of pronase-treated monolayers was 3.17 times higher than that after infection of control cells (Table 1).

Cell surface treatment with neuraminidase enhanced slightly the binding of both IMV and EEV. Whereas IMV binding and infectivity were increased by about 15% (Table 1), a greater effect was observed with EEV, where both binding and infectivity were increased by about 50% (Table 1).

Treatment with each enzyme therefore produced different effects on IMV and EEV, suggesting that these virions bind to different receptors. In support of this, IMV and EEV also bound to different cell lines with various efficiencies (Table 1). In contrast to IMV, the efficiency of EEV binding was not constant for the cell lines tested. If IMV and EEV bind to an identical receptor, any variation in the expression of this putative receptor between different cell lines should affect IMV and EEV binding to the same extent. On the other hand, if IMV and EEV bind to separate receptors, the efficiency of IMV and EEV binding is expected to fluctuate independently between different cell lines. The results obtained with mock-treated cells showed that the numbers of IMV counted on the cell surface for the three cell lines tested were similar (Table 1). Both sources of IMV (purified IMV and fresh EEV) led to this observation. In contrast, the efficiency of EEV binding varied between cell lines. Statistically different numbers of EEV were detected on the surface of the three cell lines infected with fresh EEV (Table 1). For example, 4.9 times more EEV was detected on BS-C-1 cells than on RK_{13} cells. This

Downloaded from http://jvi.asm.org/ on September 15, 2019 by guest

TABLE 1. Effects of incubating cells with different enzymes on the abilities of cells to support IMV and EEV binding and infectivity[a]

Cell line	Inoculum	Binding assay[b]								Infectivity assay[c]			
		Mock		Trypsin		Pronase		Neuraminidase					
		IMV	EEV	IMV	EEV	IMV	EEV	IMV	EEV	Mock	Trypsin	Pronase	Neuraminidase
BS-C-1	Purified IMV	2,104 ± 157 (100)	NA[d]	NA	NA	NA	NA	2,693 ± 93 (128)	NA	100 ± 6	NA	NA	109 ± 4
	Fresh EEV	225 ± 40 (100)	3,984 ± 155 (100)	NA	NA	NA	NA	272 ± 21 (121)	4,103 ± 243 (103)	100 ± 2	NA	NA	96 ± 3
RK_{13}	Purified IMV	2,115 ± 91 (100)	NA	2,270 ± 113 (107)	NA	169 ± 23 (8)	NA	2,407 ± 83 (114)	NA	100 ± 4	105 ± 3	10 ± 2	116 ± 5
	Fresh EEV	247 ± 29 (100)	814 ± 31 (100)	274 ± 23 (111)	1,618 ± 37 (199)	8 ± 7 (3)	2,393 ± 172 (294)	272 ± 20 (110)	1,136 ± 116 (139)	100 ± 3	230 ± 29	317 ± 34	155 ± 9
HeLa	Purified IMV	2,207 ± 57 (100)	NA	2,106 ± 134 (95)	NA	58 ± 13 (3)	NA	2,583 ± 105 (117)	NA	NA	NA	NA	NA
	Fresh EEV	317 ± 27 (100)	538 ± 53 (100)	321 ± 23 (101)	1,094 ± 122 (203)	21 ± 4 (7)	1,467 ± 136 (272)	311 ± 39 (98)	877 ± 109 (163)	NA	NA	NA	NA

[a] For binding and infectivity assays, adherent cells were grown in a 1-well culture chamber slide (Nunc) and 6-well cluster dishes (Falcon), respectively. For HeLa cells, both enzyme treatments and infections were performed in suspension (10^6 cells/ml).

[b] Mock- and enzyme-treated cells were infected on ice for 1 h (0.5 ml per 1-well chamber slide) with either purified IMV (MOI of 10 PFU/cell) or fresh EEV (MOI of 5.2 PFU/cell, with 78% resistant to MAb 5B4/2F2 neutralization) diluted in PBS–2% FBS. After being washed, cells were treated as described in the text to reveal IMV and EEV virions by double immunofluorescent staining. The numbers of IMV and EEV virions bound on the surfaces of 200 cells were then determined by confocal-microscopy examination. The data are the averages ± SDs for triplicate measures. Parenthetical data are the results expressed as percentages of the control.

[c] Mock- and enzyme-treated cell monolayers were infected on ice (0.5 ml per well of 6-well cluster dishes) for 1 h with either purified IMV or fresh EEV (containing MAb 5B4/2F2; final dilution, 1/2,560) diluted in PBS–2% FBS to obtain approximately 200 plaques per well on mock-treated monolayers. After being washed, cells were overlaid with CMC, and the plaques were counted 2 days later. The data are expressed as percentages of the control and are averages ± SDs for duplicate cultures.

[d] NA, not applicable.

observation could not be an artifact because in the same virus sample (fresh EEV), the number of IMV particles bound was similar (Table 1). The differences in EEV binding efficiency between BS-C-1 and RK_{13} cells were also confirmed by infectivity assays (data not shown). When an identical dilution of fresh EEV containing MAb 5B4/2F2 was plaqued concurrently on BS-C-1 and RK_{13} cells, the number of EEV plaques generated on a BS-C-1 monolayer was about five times greater than the number observed with RK_{13}, whereas the numbers of plaques generated by purified IMV on BS-C-1 and RK_{13} cells were similar (data not shown).

The data in Tables 1 and 2 obtained with mock-treated BS-C-1 cells also enabled the determination of the proportion of virus particles bound to cells that gave rise to a plaque. For IMV, 2,104 virions bound to 200 cells at a multiplicity of infection (MOI) of 10 [(2104/200)/10 = 1.052; that is, every IMV particle that bound formed a plaque]. However, for EEV this was not so [(3,984/200)/(5.2 × 0.78) = 4.9; that is, only 1 in every 5 EEV virions produced a plaque].

MAb B2 bound on the cell surface does not affect either EEV binding or infectivity. Recently, Chang et al. showed that MAb B2 bound to the cell surface inhibits the binding and consequently infectivity of IMV (5), suggesting that MAb B2 recognizes an IMV receptor. If IMV and EEV bind to an identical receptor, MAb B2 would also be expected to affect EEV binding and infectivity. This was addressed with BS-C-1, RK_{13}, and HeLa cells, and the results are presented in Table 2.

The preincubation of BS-C-1, RK_{13}, and HeLa cells with MAb B2 did not affect the binding of EEV. Statistically similar numbers of EEV particles were observed on the surfaces of cells pretreated with MAb B2 or culture medium (Table 2). The results of infectivity assays performed with BS-C-1 and RK_{13} cells led to an identical conclusion; similar numbers of plaques were observed independently of the preincubation treatment (Table 2).

As described by Chang et al., we observed that MAb B2 bound to the cell surface reduced IMV binding and infectivity. When BS-C-1 cells were preincubated with MAb B2 and subsequently infected with purified IMV, the binding and plaque formation of IMV were reduced by 83 and 77%, respectively (Table 2 [purified IMV used as the inoculum]). A similar inhibition of IMV binding was observed when fresh EEV was used as the inoculum (81% [Table 2]). The results obtained with RK_{13} cells were qualitatively similar; however, the percentage of inhibition was lower than that for BS-C-1 cells. Importantly, with both cell lines, MAb B2 inhibition of IMV binding was not total. This partial inhibition may be explained either by the existence of more than one IMV receptor or by the inability of the MAb B2 supernatant to saturate all MAb B2-reactive epitopes on the cell surface. The second possibility was eliminated, since after a first incubation with BS-C-1, RK_{13}, or HeLa cells, the MAb B2 supernatant fully retained its ability to reduce IMV binding when it was applied to fresh cells (data not shown).

Effect of MAb B2-reactive receptor capping on EEV binding. These data suggested that the MAb B2-reactive receptor is involved in IMV binding but not EEV binding. However, it remained possible that IMV and EEV bind to different domains of MAb B2-reactive receptor and that the IMV domain was neutralized by MAb B2 while the EEV domain was not. To test this possibility, we induced the capping of MAb B2-reactive receptor and investigated its effect on EEV binding.

Despite several attempts, we were not able to induce proper capping of MAb B2-reactive receptor in BS-C-1 or RK_{13} cells (data not shown). This could be attributed to their adherent phenotype. In contrast, capping was successfully induced in

Downloaded from http://jvi.asm.org/ on September 15, 2019 by guest

TABLE 2. Effects of MAb B2 on the abilities of cells to support IMV and EEV binding and plaque formation[a]

Cell line	Inoculum	Binding assay[b]				Infectivity assay[c]	
		Mock		MAb B2		Mock	MAb B2
		IMV	EEV	IMV	EEV		
BS-C-1	Purified IMV	2,057 ± 87 (100)	NA[d]	350 ± 34 (17)	NA	100 ± 4	23 ± 2
	Fresh EEV	241 ± 26 (100)	3,278 ± 122 (100)	46 ± 25 (19)	3,245 ± 87 (99)	100 ± 4	106 ± 7
RK_{13}	Purified IMV	2,103 ± 89 (100)	NA	878 ± 82 (42)	NA	100 ± 6	35 ± 5
	Fresh EEV	268 ± 20 (100)	687 ± 39 (100)	136 ± 43 (51)	701 ± 73 (102)	100 ± 4	96 ± 7
HeLa	Purified IMV	2,198 ± 110 (100)	NA	474 ± 22 (22)	NA	NA	NA
	Fresh EEV	294 ± 33 (100)	483 ± 62 (100)	55 ± 8 (19)	466 ± 35 (97)	NA	NA

[a] For binding and infectivity assays, adherent cells were grown in a 1-well culture chamber slide (Nunc) and 6-well cluster dishes (Falcon), respectively. For HeLa cells, both incubations (10^6 cells/0.2 ml) and infections (10^6 cells/ml) were performed in suspension. Before infection, cells were incubated with undiluted MAb B2 supernatant (450 μl per 1-well chamber slide or per well of 6-well cluster dishes) or with MEM–10% FBS (mock-treated cells) for 1 h on ice and then extensively washed with cold PBS–2% FBS.

[b] Mock- and MAb B2-treated cells were infected on ice for 1 h with either purified IMV (MOI of 10 PFU/cell) or fresh EEV (MOI of 4.6 PFU/cell, with 74% resistant to MAb 5B4/2F2 neutralization) diluted in PBS–2% FBS. After being washed, cells were treated as described in the text to reveal IMV and EEV virions by double immunofluorescent staining. The numbers of IMV and EEV virions bound on the surfaces of 200 cells were then determined by confocal-microscopy examination. The data are the averages ± SDs for triplicate measures. Parenthetical data are the results expressed as percentages of the control.

[c] Mock- and MAb B2-treated cell monolayers were infected on ice for 1 h with either purified IMV or fresh EEV (containing MAb 5B4/2F2; final dilution, 1/2,560) to obtain approximately 200 plaques per well on mock-treated monolayers. After being washed, cells were overlaid with CMC, and the plaques were counted 2 days later. The data are expressed as percentages of the control and are averages ± SDs for duplicate cultures.

[d] NA, not applicable.

HeLa cells grown in suspension by the protocol described in Materials and Methods.

To visualize and to control capping, cells were fixed before (Fig. 3A, panel b) or after (Fig. 3A, panel c) incubation at 37°C for 10 min. MAb B2/RAM-IgM complexes were then revealed by FITC-conjugated goat anti-rabbit IgG (GARB). Before the 37°C incubation period, the distribution of MAb B2-reactive epitope on the cell surface was mostly diffuse despite the presence of several small clusters (Fig. 3A, panel b). These clusters were artifacts of the three-step staining procedure (MAb B2, RAM-IgM, and FITC-GARB) as they were not observed when cells were subjected to indirect immunofluorescent staining with MAb B2 followed by FITC-SAM-IgM (data not shown). However, after 10 min at 37°C, all the FITC fluorescence was clustered, indicating capping of MAb B2-reactive receptor (Fig. 3A, panel c). The specificity of MAb B2 staining was controlled by using an irrelevant mouse IgM MAb as the primary antibody (Fig. 3A; compare panels a and b).

To address the effect of MAb B2-reactive receptor capping on EEV binding, the following three preparations of HeLa cells were subjected to the binding assay (Fig. 3B): (i) cells preincubated with an irrelevant mouse IgM MAb (negative control cells) (panel a), (ii) cells treated as described in Materials and Methods to induce MAb B2-reactive receptor capping but with omission of the 10-min incubation period at 37°C (MAb B2-labelled cells) (panel b), and (iii) cells treated to induce capping of MAb B2-reactive receptor (MAb B2-capped cells) (panel c).

Figure 3B shows that the capping of MAb B2-reactive receptor did not affect EEV binding, since similar numbers of EEV particles were observed on the surfaces of negative control, MAb B2-labelled, and MAb B2-capped cells. The capping of MAb B2-reactive receptor did not increase the degree to which IMV binding was inhibited by MAb B2, since similar numbers of particles were observed on cells whether or not capping was induced (Fig. 3B; compare panels b and c).

The capping of MAb B2-reactive receptor very probably reduces access to any part of this receptor by steric inhibition. The observation that EEV binding was not affected by the capping of MAb B2-reactive receptor might be explained in two ways. Either MAb B2-reactive receptor is not involved in EEV binding or EEV is able to bind to MAb B2-reactive receptor despite its capping. If the latter was true, EEV binding sites and MAb B2-reactive molecule clusters would colocalize on the surfaces of MAb B2-capped cells. To test this, we used a double immunofluorescent staining to visualize simultaneously MAb B2-reactive molecule clusters and EEV (Fig. 4). One hundred cells, containing 254 bound EEV, were examined by confocal microscopy to determine the relative localization of EEV binding sites and MAb B2-reactive molecule clusters. All but six EEV particles (which were observed at the periphery of MAb B2-reactive molecule clusters) were present at positions clearly isolated from the MAb B2 clusters, and three representative cells are shown in Fig. 4.

MAb B2 prevents IMV binding by steric inhibition. Chang et al. have shown that the MAb B2-reactive epitope is sensitive to trypsin digestion (5). However, these data did not determine the effect of trypsin digestion on IMV binding. Table 1 shows that cell surface trypsin digestion does not affect IMV binding, suggesting that the MAb B2-reactive epitope is not the IMV binding site and consequently that MAb B2 prevents IMV binding by steric inhibition. To be certain about this, it was necessary to demonstrate that trypsin digestion destroyed all of the MAb B2-reactive epitope present on the cell surface. To examine this, the MAb B2-reactive epitope on the surfaces of mock-digested and trypsin-digested cells was quantified by indirect immunofluorescent staining and flow cytometry (Fig. 5). Trypsin-treated cells had a relative fluorescence intensity identical to that of negative control cells (mock-treated cells stained with an irrelevant mouse IgM MAb as the primary antibody), indicating that the great majority of MAb B2-reactive epitopes were destroyed after trypsin treatment (Fig. 5). As this treatment has no effect on IMV binding, the mechanism by which MAb B2 prevents IMV binding must be steric inhibition.

DISCUSSION

VV produces two types of infectious particles, IMV and EEV. EEV is an IMV particle with an additional outer membrane that contains proteins that are absent from IMV. This EEV outer membrane explains why IMV-neutralizing antibodies fail to inhibit the infectivity of EEV particles (15). The EEV outer membrane has been described as a loose and extremely

Downloaded from http://jvi.asm.org/ on September 15, 2019 by guest

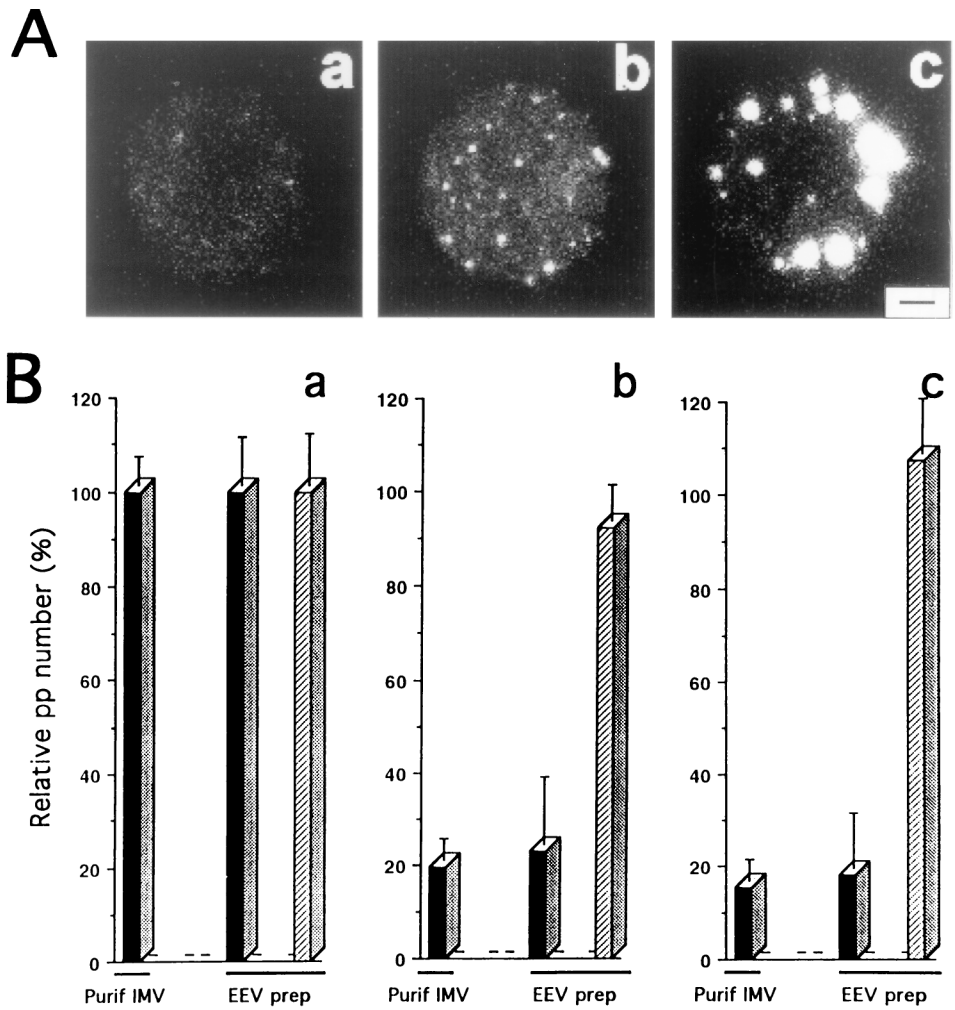

FIG. 3. (A) Capping of MAb B2-reactive receptor. HeLa cells grown as suspension cultures were processed as described in Materials and Methods to induce capping of MAb B2-reactive molecules (b and c). To visualize capping, cells were fixed before (b) or after (c) incubation at 37°C for 10 min and MAb B2/RAM-IgM complexes were revealed by FITC-GARB (12 μg/10^6 cells in 0.2 ml of PBSF). (a) Cell incubated with an irrelevant primary mouse IgM MAb and then treated as described for panel b. Bar, 2 μm. (B) Effect of MAb B2-reactive receptor capping on EEV binding. The following three preparations of HeLa cells were subjected to the binding assay: cells preincubated for 45 min at 0°C with an irrelevant mouse IgM MAb (Serotec) (10 μg/10^6 cells per 0.2 ml of PBSF) (negative control cells) (a), cells treated as described in Materials and Methods to induce MAb B2-reactive receptor capping without incubation at 37°C for 10 min (MAb B2-labelled cells) (b), and cells treated to induce capping of MAb B2-reactive receptor (MAb B2-capped cells) (c). These three cell preparations were then infected (10^6 cells/ml) on ice for 1 h with either purified (Purif) IMV (MOI of 10 PFU/cell) or fresh EEV (EEV prep) (MOI of 5.1 PFU/cell, with 79% resistant to neutralization by MAb 5B4/2F2) diluted in PBS–2% FBS. After being washed with PBS–2% FBS to remove unadsorbed virus, cells were treated as described in the text to reveal virions by double indirect immunofluorescent staining. The numbers of IMV (black bars) and EEV (hatched bars) virions bound on the surfaces of 200 cells were then determined by confocal-microscopy examination. Data are expressed as percentages of the control and are the averages ± SDs for triplicate measures. For control cells infected with purified IMV, a mean of 2,253 IMV virions was observed. For control cells infected with fresh EEV, means of 217 IMV virions and 509 EEV virions were observed. pp, physical particle.

fragile structure, and even when virions from the supernatant of infected cells were analyzed by cryoelectron microscopy, only a minority of particles had a complete and intact outer membrane (16). The data presented here show that the purification of EEV leads to the isolation of a majority of particles with a damaged outer membrane, as revealed by their sensitivity to a MAb that neutralizes IMV. Similar observations have been published recently by Ichihashi (9), who showed that treatments such as sonication and one cycle of freeze-thawing were sufficient to rupture the EEV membrane. Because damaged EEV could bind to the cell via an EEV or IMV protein, purified EEV should not be used for binding studies.

We took advantage of the fact that VV virions are very large to visualize them by fluorescent microscopy (conventional or confocal) after chemical (DNA labelling with DAPI) or indirect immunofluorescent labelling. The ability to visualize individual particles was then exploited to develop an original binding assay using double indirect immunofluorescence to differentiate and count IMV and EEV bound to the cell surface by confocal-microscopy analysis. This binding assay has several useful features. (i) By its capacity to reveal and identify simultaneously IMV and EEV, it enables unpurified preparations containing both forms of VV to be used. (ii) This assay does not require any prelabelling of the virus. (iii) The results generated are absolute numbers of virus particles/cell, not relative numbers representing the mean score of the cell culture; therefore, this assay could identify which cells in a heterogenous culture bind IMV and/or EEV even if only a small fraction of cells do so. (iv) The assay gives steric information concerning the location of the virus binding site on the cell. (v)

Downloaded from http://jvi.asm.org/ on September 15, 2019 by guest

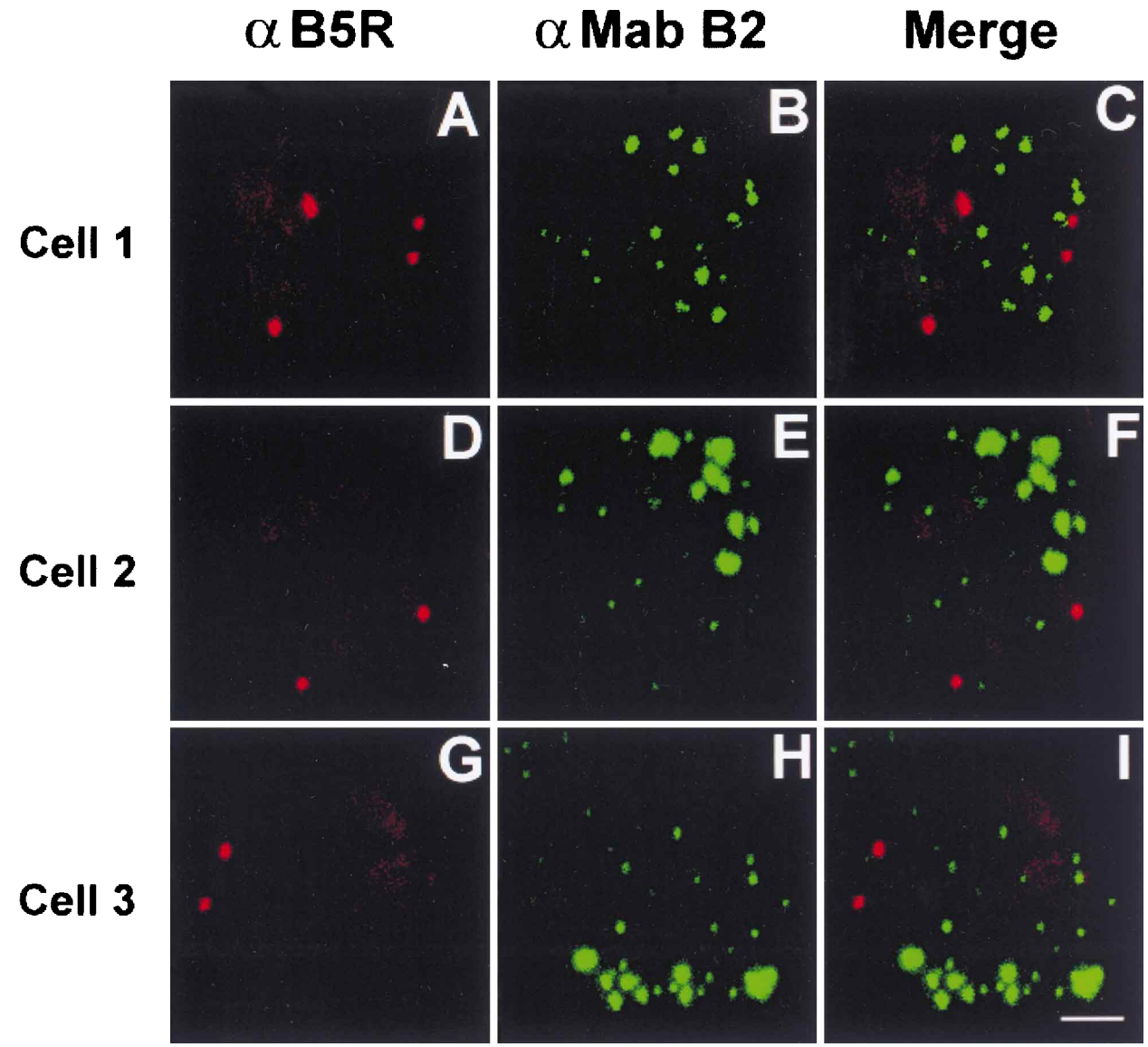

FIG. 4. Concomitant detection of EEV (red signal) and MAb B2-reactive molecule clusters (green signal) on the surfaces of HeLa cells. HeLa cells were grown as suspension cultures and were processed as described in Materials and Methods to induce capping of MAb B2-reactive molecules. Cells were then infected with fresh EEV at the MOI of 3.5 EEV PFU/cell (10^6 cells/ml) on ice for 1 h. After being washed with cold PBS–2% FBS, cells were fixed in PBS containing 4% paraformaldehyde (wt/vol) for 20 min on ice. MAb B2/RAM-IgM complexes were revealed by FITC-GARB. EEV were revealed by indirect immunofluorescent staining with MAb 19C2 as the primary antibody and PE-RAR as the secondary antibody. Cells were first incubated simultaneously with FITC-GARB and MAb 19C2 for 45 min at 37°C and after being washed were incubated with PE-RAR at 37°C for 30 min. After final washing, cells were mounted and examined by confocal microscopy. The three horizontal rows are analyses of three different cells. The first and second panels of each line are the emissions of red and green fluorescences, respectively, and the third panel is the merged image of the red and green emissions. Bar, 2 μm.

It enables staining with three or more antibodies, providing a way to investigate any correlation between the expression of a particular receptor and the capacity of a cell to bind EEV or IMV in a mixed cell population.

By this binding assay, we have shown that IMV and EEV bind to different cellular receptors. This conclusion is based on three observations. (i) The efficiencies with which different cell lines bind EEV and IMV are unrelated, (ii) cell surface treatments with some enzymes affect IMV and EEV binding differently, and (iii) MAb B2 bound on the cell surface does not affect EEV binding, even after capping of the unidentified molecule to which it binds.

In regard to the capacities of different cell lines to support EEV and IMV binding, we observed that while BS-C-1, RK_{13}, and HeLa cells bound IMV with similar efficiencies, these cells showed considerable variation in their capacities to bind EEV (Table 1), suggesting that the two forms of VV bind to different receptors. Theoretically, it should be possible to find cell lines which support exclusively IMV or EEV binding or cell lines which do not support the binding of IMV and EEV. These cell lines might be very useful in identifying IMV and EEV receptors by screening expression libraries of cDNA.

Cell surface treatments with trypsin, pronase, and neuraminidase affected IMV and EEV binding in different ways. The most spectacular effect was observed with pronase treatment, which nearly abolished IMV binding while EEV binding was

Downloaded from http://jvi.asm.org/ on September 15, 2019 by guest

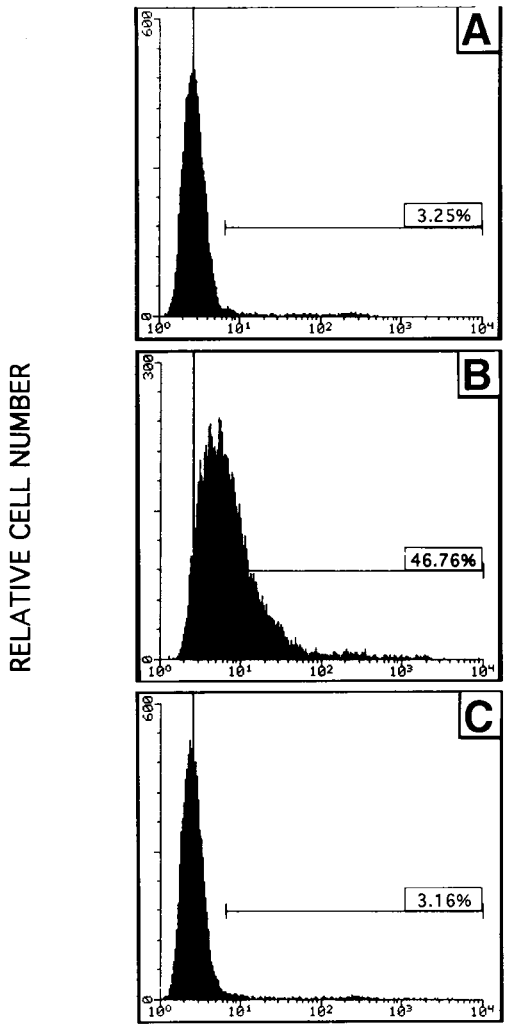

FIG. 5. MAb B2-reactive epitope is removed from the cell surface after trypsin treatment. HeLa cells grown as suspension cultures were mock (A and B) or trypsin (C) treated as described in Materials and Methods. Cell surface MAb B2-reactive epitope was quantified by flow cytometry. (A) Background staining of mock-treated cells stained with a mouse isotype IgM negative control and with secondary antibody. (B and C) Mock- and trypsin-treated cells stained for detection of MAb B2-reactive epitope, respectively.

enhanced (Table 1). This result showed that the IMV receptor must be composed of a peptide. The fact that pronase treatment seems to increase the accessibility of the EEV receptor does not prove that this receptor is not a protein; it could be a protein strongly resistant to protease treatment.

Lastly, the binding of MAb B2 to the cell surface, which inhibits IMV binding, has no effect on EEV binding, even after capping of the MAb B2-reactive molecule, indicating that this molecule is not a binding receptor for EEV. As to the inhibition of IMV binding by MAb B2, our results broadly confirm those published by Chang et al. (5), except that the degree to which IMV binding was prevented by MAb B2 was slightly different and that complete inhibition was not achieved. These results suggest that although the molecule recognized by MAb B2 is the major IMV receptor, it is not the only IMV receptor. Finally, our data demonstrate that MAb B2 prevents IMV binding by steric inhibition, because although trypsin treatment destroyed MAb B2 binding to cells, IMV binding was not affected.

Although saturation binding experiments were not possible due to the low concentration of EEV in fresh supernatants, we believe that the binding of virions to cells was specific. First, every bound IMV gave rise to a plaque, whereas for EEV only one in five virions did so. Second, the use of different cell types and the treatment of cells with three enzymes or MAb B2 affected the binding of IMV and EEV to cells and their infectivity to the same degree. If some binding was nonspecific, this would not have been so.

VV (and other orthopoxviruses) are unusual in that they produce two types of infectious virions, with different structures, antigenicity and biological properties. This is probably advantageous to the virus in enabling transmission in different ways but may also broaden the cell, tissue, or host tropism. The determination of the extent to which tropism may be broadened will require the identification of the IMV and EEV receptors and an analysis of their distribution. In vivo it may be that some cells express preferentially or exclusively IMV or EEV receptors. Consistent with this possibility, an analysis of only three cell lines has already shown considerable variation in EEV binding (Table 1). Another complication is that there is more than one IMV receptor, since MAb B2 only partially inhibited IMV binding (Table 2). Possibly EEV will also have several cellular receptors that are bound by different EEV glycoproteins.

In conclusion, we have described a novel method based on confocal microscopy to study virus binding. This assay has been applied to the study of VV binding, a field which has hitherto been complicated by the existence of two structurally and antigenically distinct forms of virus (IMV and EEV) which have not been physically purified from each other without damaging the outer envelope of EEV. Although the utility of this technique has been demonstrated here with VV, it should be applicable to any virus that is larger than 50 nm.

ACKNOWLEDGMENTS

We are most grateful to Christopher M. Sanderson for ideas and advice with capping experiments. MAb B2 was kindly provided by Wen Chang (Chinese Culture University, Republic of China). MAb 5B4/2F2 was a gift from Claus P. Czerny (Institute of Medical Microbiology, Infectious and Epidemic Diseases, Ludwig-Maximilians-University, Munich, Germany).

A. Vanderplasschen is a senior research assistant of the Fonds National Belge de la Recherche Scientifique (F.N.R.S.) and is the laureate of a NATO research fellowship. This work was supported by program grant PG8901790 from the U.K. Medical Research Council.

REFERENCES

1. **Appleyard, G., and C. Andrews.** 1974. Neutralizing activities of antisera to poxvirus soluble antigens. J. Gen. Virol. **23:**197–200.
2. **Appleyard, G., A. J. Hapel, and E. A. Boulter.** 1971. An antigenic difference between intracellular and extracellular rabbitpox virus. J. Gen. Virol. **13:**9–17.
3. **Boulter, E. A.** 1969. Protection against poxviruses. Proc. R. Soc. Med. **62:** 295–297.
4. **Boulter, E. A., and G. Appleyard.** 1973. Differences between extracellular and intracellular forms of poxviruses and their implications. Prog. Med. Virol. **16:**86–108.
5. **Chang, W., J.-C. Hsiao, C.-S. Chung, and C.-H. Bair.** 1995. Isolation of a monoclonal antibody which blocks vaccinia virus infection. J. Virol. **69:**517–522.
6. **Cook, P. R., and I. A. Brazell.** 1975. Supercoils in human DNA. J. Cell Sci. **19:**261–279.
7. **Czerny, C. P., and H. Mahnel.** 1990. Structural and functional analysis of orthopoxvirus epitopes with neutralizing monoclonal antibodies. J. Gen. Virol. **71:**2341–2352.
8. **Essani, K., and S. Dales.** 1979. Biogenesis of vaccinia: evidence for more

Downloaded from http://jvi.asm.org/ on September 15, 2019 by guest

than 100 polypeptides in the virion. Virology **95:**385–394.
9. **Ichihashi, Y.** 1996. Extracellular enveloped vaccinia virus escapes neutralization. Virology **217:**478–485.
10. **Ichihashi, Y., S. Matsumoto, and S. Dales.** 1971. Biogenesis of poxviruses: role of A-type inclusions and host cell membranes in virus dissemination. Virology **46:**507–532.
11. **Mackett, M., G. L. Smith, and B. Moss.** 1985. The construction and characterization of vaccinia virus recombinants expressing foreign genes, p. 191–211. *In* D. M. Glover (ed.), DNA cloning: a practical approach. IRL Press, Oxford, United Kingdom.
12. **McIntosh, A. A. G., and G. L. Smith.** 1996. Vaccinia virus glycoprotein A34R is required for infectivity of extracellular enveloped virus. J. Virol. **70:**272–281.
13. **Parkinson, J. E., and G. L. Smith.** 1994. Vaccinia virus gene A36R encodes a Mr 43-50K protein on the surface of extracellular enveloped virus. Virology **204:**376–390.
14. **Payne, L. G.** 1979. Identification of the vaccinia hemagglutinin polypeptide from a cell system yielding large amounts of extracellular enveloped virus. J. Virol. **31:**147–155.
15. **Payne, L. G.** 1980. Significance of extracellular enveloped virus in the *in vitro* and *in vivo* dissemination of vaccinia virus. J. Gen. Virol. **50:**89–100.
16. **Roos, N., M. Cyrklaff, S. Cudmore, R. Blasco, J. Krijnse-Locker, and G. Griffiths.** 1996. A novel immunogold cryoelectron microscopic approach to investigate the structure of the intracellular and extracellular forms of vaccinia virus. EMBO J. **15:**2343–2355.
17. **Sanderson, C. M., J. E. Parkinson, M. Hollinshead, and G. L. Smith.** 1996. Overexpression of the vaccinia virus A38L integral membrane protein promotes Ca^{2+} influx into infected cells. J. Virol. **70:**905–914.
18. **Schmelz, M., B. Sodeik, M. Ericsson, E. J. Wolffe, H. Shida, G. Hiller, and G. Griffiths.** 1994. Assembly of vaccinia virus: the second wrapping cisterna is derived from the trans Golgi network. J. Virol. **68:**130–147.
19. **Turner, G. S., and E. J. Squires.** 1971. Inactivated smallpox vaccine: immunogenicity of inactivated intracellular and extracellular vaccinia virus. J. Gen. Virol. **13:**19–25.
20. **Vanderplasschen, A., M. Goltz, J. Lyaku, C. Benarafa, H.-J. Buhk, E. Thiry, and P.-P. Pastoret.** 1995. The replication *in vitro* of the gammaherpesvirus bovine herpesvirus 4 is restricted by its DNA synthesis dependence on the S phase of the cell cycle. Virology **213:**328–340.

Downloaded from http://jvi.asm.org/ on September 15, 2019 by guest